Invariance of the Dissipative Action at Ultrahigh Strain Rates Above the Strong Shock Threshold

Jonathan C. Crowhurst, Michael R. Armstrong, Kimberly B. Knight, Joseph M. Zaug, and Elaine M. Behymer

Phys. Rev. Lett. **107**, 144302 — Published 30 September 2011

DOI: 10.1103/PhysRevLett.107.144302

Invariance of the Dissipative Action at Ultrahigh Strain Rates above the Strong Shock Threshold

Jonathan C. Crowhurst*†, Michael R. Armstrong†, Kimberly B. Knight, Joseph M. Zaug, Elaine M. Behymer

Physical and Life Sciences Directorate, Lawrence Livermore National Laboratory, Livermore,

California 94550, USA

*** crowhurst1@llnl.gov**

†These authors contributed equally to this work.

We have directly resolved shock structures in pure aluminum in the first few hundred picoseconds subsequent to a dynamic load, at peak stresses up to 43 GPa and strain rates of in excess of 10^{10} s^{-1}. For strong shocks we obtain peak stresses, strain rates, and rise times. From these data, we directly validate the invariance of the dissipative action in the strong shock regime, and by comparing with data obtained at much lower strain rates show that this invariance is observed over at least 5 orders of magnitude in the strain rate. Over the same range, we similarly validate the fourth-power scaling of strain rate with peak stress (the Swegle-Grady relation).

Controlled shock compression[1] has been used for decades to examine the behavior of materials under extreme conditions of pressure and temperature. In solids, a sufficiently large amplitude shock produces irreversible plastic deformation and relaxes the initial anisotropic stress. As the amplitude continues to increase, and if the shock drive is maintained, a steady-wave shock profile evolves, which propagates indefinitely without change in form[2]. This steadiness is due to the attainment of a stable balance between the competing effects of a nonlinear stress-strain response and dissipative or viscous material behavior[3,4] (tending to steepen and broaden the shock profile, respectively). However, despite its importance in numerous contexts a fundamental understanding of shock-induced deformation is still lacking. In particular, little is understood about the behavior of materials, including metals[5], during the initial phase of shock compression and at high strain rates[6]. To a large extent this is a consequence of the relevant time scale which becomes extremely short at even quite small shock stresses[7]. Thus shock wave profiles, although retaining finite rise times, often cannot be sufficiently well resolved to permit quantitative conclusions. A relevant example is shock compression in aluminum. Despite it being a very commonly studied and employed metal in shock wave experiments, there are no directly relevant data above strain rates of ~ 10^7 s^{-1}, and recent theoretical models are still compared to data obtained 40 years ago[18,19,4]. We note too that such low strain rates correspond to stresses well below the strong

shock threshold, or overdriven stress, σ_O. This historical lack of sufficient time resolution[20] has precluded testing, at high strain rates, potentially fundamental scaling laws whose verification depend directly on the ability to resolve shock wave profiles. These include one of the most general thus far observed which is that the product of the specific energy dissipated by the shock and the time over which this takes place, is invariant[4]. As suggested by the discussion of Grady[4], we refer to this product as the dissipative action, A.

Within the last 15 years, very high time resolution has been achieved using laser-based techniques[8,10-17], however a physical picture of plasticity that is clearly consistent or inconsistent with longer time scale experiments has not yet emerged. Here we measure shock rises in aluminum above σ_O, and obtain shock stresses, shock widths, and strain rates. We use these data to test the validity, at ultrahigh strain rates, of the invariance of the dissipative action as well as related scaling laws such as the fourth power dependence of the strain rate, $\dot{\eta}$, on the shock stress, σ.

For a well-defined and steady shock, equation of state data may be inferred from measured values of the shock and particle velocities, u_s and u_p, respectively, via the Rankine-Hugoniot relations[1] . In the case of an optical technique[15] and a metal sample this implies measurement of the propagation time of the shock through the sample and of the time history of the position of the metal surface in response to the arrival of the shock. A schematic of the experiment is shown in Figure 1. The arrival time of a shock at the free surface of the lower step (of thickness $h_1 = 0.72$ μm) is first measured (in Position 1 of Fig. 1) to establish the time of injection of the nominally well-defined and fully steepened shock into the upper step (of total thickness $h_2 = 1.44$ μm). This approach minimizes spatial and temporal uncertainties associated with the formation of the shock due to plasma expansion which occurs over some finite but unknown depth. Another shock, in a separate shot, is then launched towards the surface of the upper step (Position 2)[21-23].

Figure 2 shows two sets of free surface velocity (u_{fs}) histories for different pump pulse energies. Pump energy is larger for the histories of Fig. 2(a). The histories of Fig. 2(a) obtained at the two free surfaces (i.e Positions 1 and 2 of Fig. 1) are qualitatively similar; the initial rise in particular has the same simple shape. This rise is consistent with a one-wave shock structure in which the plastic shock has overtaken the elastic precursor, i.e. a strong or overdriven shock. Data of this type allow independent determination of u_p and u_s and thus shock stress and density. To determine u_p, we assumed $u_p = u_{fs}/2$ and obtained the maximum value of $u_p$by inspection of the initial rise[22]. To determine u_s, we divided the difference in step thickness, $h_2 - h_1$, by the difference in arrival times of the two rises (Fig. 4 of Ref 22). The time resolution is also sufficient to allow estimation, by inspection, of the rise time, Δt, and thus the plastic shock width, $w = u_s \times \Delta t$. Furthermore, the slope of the linear part of the rise yields $\dot{u}_p^{max}$ (Fig. 5, Ref. 24) and thus the strain rate, $\dot{\eta} = \dot{u}_p^{max}/u_s$. Fig. 2(b) by contrast shows structured rises whose shapes depend on propagation distance. These data are discussed in more detail in Ref. 22; here we analyze strong shocks (Table 1, Ref. 22) with the structure shown in Fig. 2(a) in order to make comparisons with the known Hugoniot of aluminum (Fig. 6 of Ref. 22, which shows our data for $u_p$and u_s and reported values for 1100 Al[24,25] and 6061 Al[24]. Average deviations of our steady data from the relation[24] for 1100 Al of $u_s = 5.38 + 1.34u_p$ are less than a percent.). We note that the stress at which we clearly observe one wave structures yields a lower limit for σ_O; specifically for propagation distances of 1.44 μm after initiation in aluminum, the overdriven threshold exceeds ~ 25 GPa. This may be compared with the value obtained by intersecting the known u_p- u_s relation with a constant elastic wave speed of 6.41 km s^{-1} of ~ 13.3 GPa (see note in Ref. 24).

In Figure 3 we compare our measured widths to theoretical calculations for 6061-T6 Al by Molinari and Ravichandran[18]. The latter considered shock stresses in the range of 1 GPa to 15 GPa. By combining these results with ours we see that from 1 GPa to ~ 43 GPa the shock width decreases from ~ 10-20 cm

to ~ 0.2 micrometers, i.e. by a factor of more than 10^5! This implies that above 40 GPa the shock is fully risen within several hundred atomic layers. On the basis of work by Bland[26], Swegle and Grady[3] define the dimensionless Bland number, $B = 3hs\dot{\eta}/8c$, where h is the sample thickness, and s and c are the slope and the intercept respectively of the u_p- u_s relation. For $B > 1$ steady wave conditions may be expected to hold with some confidence but for smaller values steady wave conditions are doubtful[3]. Our overdriven data shown in Figure 3 have B mostly larger than one (Table 1, Ref. 22. For this calculation and all those that follow we assumed c = 5.38 km s^{-1}, and s = 1.34). For propagation distances of ~ 1.5 μm, this corresponds to a minimum shock stress of ~ 30 GPa. Below this stress measured shock fronts will exhibit very large (up to ~ 10 GPa) elastic rises with fast rise times followed by slower plastic rises [Fig. 2(b)] (see also Refs. 16, 17, 29). On this basis we conclude that reported observations of plastic shocks with very small widths at anomalously low stresses[13], were in reality observations of large amplitude elastic precursors (Figure 8 of Ref. 22. See also Ref. 16).

It has been empirically observed that the strain rate of steady shocks in metals is related to the shock stress, σ, by a power law[3,4] of the form $\dot{\eta} \propto \sigma^m$, and that furthermore $m \cong 4$. As noted earlier, this relationship has been verified experimentally only at relatively low strain rates due to the fact that the experimental time resolution has historically been limited. In Figure 4 we have plotted on a log-log scale measured peak[30] shock stresses against measured strain rates for our overdriven shocks (upper panel). Also plotted is the lower strain rate data of Barker[27] for 6061-T6 Al presented by Swegle and Grady[3,28]. Remarkably, we find that the linear relationship between $\log\sigma$ and $\log\dot{\eta}$ is maintained over an enormous range of strain rates (10^5 s^{-1} to at least 10^{10} s^{-1}) and that the inverse of the corresponding slope is very close to 4. This value may be compared to the theoretical estimates of 3.3 and 3.92 (Refs. 19 and 18, respectively). We note that our lowest stress datum (at ~ 25 GPa) is substantially below the straight line trend; however it is also true that the Bland number for this point was less than one (Table

1, Ref. 22). This is consistent with the fact that the fourth-power law is expected to hold only for steady waves and is comparable to the behavior observed for shocks in vanadium[31] that were shown to be nonsteady[32,4].

As pointed out by Grady[4], the fourth-power relation was not the original expression that was proposed to be generally applicable. Instead, it had earlier been suggested that the product of the energy dissipated by the shock wave and the time over which this takes place is an invariant[33]. Whereas the fourth power law is only applicable to steady waves, the invariance applies generally to both steady and nonsteady waves[4]. Furthermore, this product has units of specific energy×time, or length^2/time and is thus consistent with (specific) action in the context of classical mechanics[4]. We test the invariance (Fig. 4, middle panel) by calculating the product $A = \varepsilon \times \Delta t$, (Eq. 5 of Grady[4]) where[33,34] $\varepsilon = [s/3\rho_0(\rho_0 c^2)^2]\sigma^3$ (Eq. 3 of Grady[4] to lowest order in $\sigma/\rho_0 c^2$). For Δt we use our measured rise times. To compare with the data of Barker[27,3] we use Eq. 4 of Grady[4] to conveniently estimate rise times for those data, i.e. $\Delta t \cong \sigma/\rho_0 c^2 \dot{\eta}$. We find indeed that both sets of data are consistent and reasonably constant despite the very large range of strain rates and corresponding energies and rise times (lower panel of Fig. 4). We note that on the linear ordinate scale of Fig. 4 (middle panel), our nonsteady point once again appears to be an outlier which may be consistent with an inapplicability of Eq. 3 of Grady[4], which was derived for steady waves, directly to nonsteady data. Finally, we consider the related dependence of the shock viscosity on strain rate as proposed by Grady[4]. Grady defines the viscosity as $\nu = \frac{1}{4} s\sigma\Delta t$ (Eq. 9 of Grady[4]). On the basis of the invariance of the dissipative action and the fourth power law we expect in turn that $\nu \propto \dot{\eta}^{-1/2}$. Figure 9 of Ref. 22 confirms this result.

In conclusion we have shown that fourth power scaling and invariance of the dissipative action hold even at ultra-high strain rates above the overdriven threshold in aluminum. Together with the

consistency of our strong shock data with the known u_p-u_s relation we also conclude that above σ_O, the dynamic behavior at early times in thin (~ 1 μm) Al films cannot be distinguished from that of much thicker (i. e. bulk) material.

Acknowledgements

We acknowledge useful discussions with L. E. Fried, B. W. Reed, R. W. Minich, N. R. Barton, D. C. Swift, J. S. Stolken, M. Kumar, P. H. Erhart, I. Oleynik, V. Zhakhovsky, N. Inogamov, A. Arsenlis, E. J. Reed, G. Ravichandran, Y.M. Gupta, W. J. Nellis, B. Sadigh, L. A. Zepeda-Ruiz, and J. Hamilton. We thank J. M. Chesser for assistance in determining thin film thicknesses. This work was performed under the auspices of the U.S. Department of Energy by Lawrence Livermore National Laboratory under Contract No. DE-AC52-07NA27344 with Laboratory directed Research and Development funding (11ERD039), as well as being based on work supported as part of the EFree, an Energy Frontier Research Center funded by the U.S. Department of Energy, Office of Science, Office of Basic Energy Sciences under Award No. DESC0001057.

References:

1. W. J. Nellis, Prog. Phys. **69**, 1479 (2006).

2. In the absence of phase transitions.

3. J. W. Swegle and D. E. Grady, J. Appl. Phys. **58**, 692, (1985).

4. D. E. Grady, J. Appl. Phys. **107**, 013506 (2010).

5. E. M. Bringa *et al*., Nature Mat. **5**, 805 (2006).

6. W. J. Murphy *et al.*, J. Phys. Cond. Mat. **20**, 065404 (2010).

7. Historically, shock waves have been mostly driven by impact of a material projectile with the sample target. The projectile is set in motion mainly using gun-type approaches[1] (chemical explosives, light gas guns, etc). Energy-based approaches have also been adopted, in particular those employing lasers[1]. Here the laser is used to launch the projectile or, alternatively, to launch a shock directly into the target, via rapid expansion of a hot dense plasma (either in the target itself or in a layer of material on the target). Using high energy lasers, extremely high shock stresses have been achieved e.g. Refs. 8,9. However, smaller scale experiments in which tight focusing somewhat compensates for relatively low energy, have also proven feasible[10-17]. Although shock waves generated by mechanical impact may have picosecond rise times, traditional techniques used to observe the shock rise do not have the time resolution to observe the onset of plasticity at high stress.

8. D. Batani *et al*., European Phys. J. D **23**, 99 (2003).

9. R. S. McWilliams *et al*., Phys. Rev. B **81**, 014111 (2010).

10. R. Evans *et al*., Phys. Rev. Lett. **77**, 3359 (1996).

11 K. T. Gahagan *et al.*, Phys. Rev. Lett. **85**, 3205 (2000).

12. J. Chen, R. Li, Z. Zeng, X. Wang, and Z. Xu, Science in China Ser. G Physics, Mechanics & Astronomy **47**, 416, (2004).

13. C. A. Bolme and D. J. Funk, Appl. Phys. A **92**, 761 (2008).

14. L. Huang, Y. Yang, Y. Wang, Z. Zheng, W. Su, J. Phys. D: Appl. Phys. **42**, 045502 (2009).

15. M. R. Armstrong, J. C. Crowhurst, S. Bastea, J. M. Zaug, J. Appl. Phys. **108**, 023511 (2010).

16. S. I. Ashitkov *et al.*, JETP Lett. **92**, 516, (2010).

17. V. H. Whitley *et al.*, J. Appl. Phys. **109**, 013505 (2011).

18. A. Molinari and G. Ravichandran, J. Appl. Phys. **95**, 1718 (2004).

19. R. A. Austin and D. L. McDowell, Int. J. Plasticity, In press, doi:10.1016/j.ijplas.2010.03.002 (2010).

20. We also note that direct comparisons with molecular dynamics simulations, which are increasingly used to model shock compression, are greatly facilitated if the experimental time resolution is consistent with the time scale of the simulations which is typically very short.

21. The method is essentially the ultrafast equivalent of the VISAR technique.

22. See EPAPS Document No. [number will be inserted by publisher] for additional discussion. For more information on EPAPS, see http://www.aip.org/pubservs/epaps.html.

23. We do not attempt to launch a single shock such that the shock front overlaps the step edge; this would permit determination of the time of injection of the actual shock used to drive the upper step free surface. Such an approach would eliminate uncertainties due to pulse energy variation; however edge effects might then become important. Fortunately, we found a degree of reproducibility from position to position that was sufficient to support the conclusions of this work.

24 S. P. Marsh, *Los Alamos Shock Hugoniot Data*, pg 165 (University of California Press, Berkeley, 1980).

25. A. C. Mitchell and W. J. Nellis, *J. Appl. Phys.* **52**, 3363 (1981).

26. D. R. Bland, J. Inst. Math. Appl. **I**, 56 (1965).

27. L. M. Barker, *Behavior of Dense Media Under High Dynamic Pressures*, pg 483 (Gordon and Breach, New York, 1968).

28. The lowest stress point of Ref. 3, had a Bland number of 0.16 but the others had Bland numbers larger than one.

29. V. V. Zhakhovskii and N. A. Inogamov, JETP Lett., **92**, 521 (2010).

30. From the point of view of modeling shock viscosity it is preferable to couch the treatment in terms of the plastic shock jump above the elastic limit rather than the peak stress; however the difference was assumed by Swegle and Grady[3] to be small for the case of (~ one cm thick) Al and was neglected.

31. L. C. Chhabildas and C. R. Hills, *Metallurgical Applications of Shock-Wave and High-Strain-Rate Phenomena*, pg 763, edited by L. E. Murr, K. P. Staudhammer, and M. A. Meyers (Dekker, New York, 1986).

32. J. W. Swegle, *Shock Compression of Condensed Matter 1991*, pg 249, edited by S. C. Schmidt, R. D. Dick, J. W. Forbes, and D. G. Tasker (Elsevier Science, New York, 1991).

33. D. E. Grady, Appl. Phys. Lett. **38**, 825, (1981).

34. The Hugoniot is assumed approximately equal to the isentrope for this derivation[33]. Although the two curves begin to deviate at ~ 30 GPa[1] this approximation appears not to have a significant effect on the present results.

Figure Legends

Fig. 1. (color online). (a) Experimental configuration used for launching and probing shock waves in pure aluminum films deposited onto glass. Part of the chirped, clipped pump pulse (~270 ps duration, centered on 800 nm, spot diameter ~20 μm, rise ~ 12 ps) is absorbed by the aluminum and consequent plasma expansion drives a shock towards the free Al surface. The time history of the motion of the free surface, (up to ~250 ps) is obtained in one shot by interfering two probe pulses (~270 ps, 800 nm, ~200 μm, separated in time by 10 ps, pulse durations not to scale) in a grating spectrometer[15]. A moving time average of 10 ps is applied to the data[22]. Measurements are made separately at the free surface of the two steps (Positions 1 and 2). Thicknesses $h_1$and h_2 are respectively ~ 0.72 μm and ~ 1.44 μm (not to scale with focal diameters).

Fig. 2. (color online). Free surface velocity histories measured at Positions 1 and 2 of Fig. 1 for decreasing pump pulse energies. The black (red) line is the numerical average of three separate shots at Position 1 (2); the thin gray lines are an example of one of the individual shots. The origin on the time axis is arbitrary. Shock rises in (a) imply a single wave structure; (b) a two wave structure containing a highly unrelaxed elastic precursor in addition to the plastic rise. Time histories correspond to shocks well above the overdriven limit (a), and below it (b). The average amplitude of the shock in (a) is ~ 40 GPa (Table 1 of Ref. 22); the average amplitude of the elastic precursor in (b) is ~ 9.2 GPa, (Table 2 of Ref. 22).

Fig. 3. (color online) Measured plastic shock widths compared to literature values. **Red squares:** widths corresponding to the present data having rises of the form shown in Fig. 2(a). **Gray triangles:** rough estimations for nonsteady shocks. Uncertainties are standard deviations for nominally fixed pump energies (hence no uncertainties quoted for single traces). **Diamonds:** calculated values for the data of

Ref. 3 that were obtained from Ref 27 for 6061-T6 Al. **Open and solid circles:** theoretical results for 6061-T6 Al of Ref. 18 with different model parameters. The black line is a fit to the solid circles and red squares only in order to permit interpolation: $\log w = 4.1e^{-\sigma/9.8} + 6.7e^{-\sigma/0.97} - 0.8$, with width in micrometers and peak stress in GPa (See Ref. 22 for further details).

Fig. 4. (color online). Dissipative action, A (triangles), rise time Δt (diamonds), dissipated specific energy ε (stars), and peak stress σ (squares), plotted against strain rate, $\dot{\eta}$. **Red symbols:** present data. **Black symbols:** strain rate data of Ref. 3 that were obtained from Ref. 27 and our corresponding calculated values for A, Δt and ε. Straight line fits to Δt, ε, and σ yield: $\log \Delta t = -2.7 - 0.78 \log \dot{\eta}$, $\log \varepsilon = -7.5 + 0.76 \log \dot{\eta}$, and $\log \sigma = -0.99 + 0.25 \log \dot{\eta}$, respectively, with Δt in s, ε in MJ kg^{-1}, σ in GPa and $\dot{\eta}$ in s^{-1}. The dashed line in the top panel is the average of all values of A except the lowest stress point of the present data (open triangle) and is equal to ~ 4.3 x 10^{-5} m^2 s^{-1}.

Figure 1.

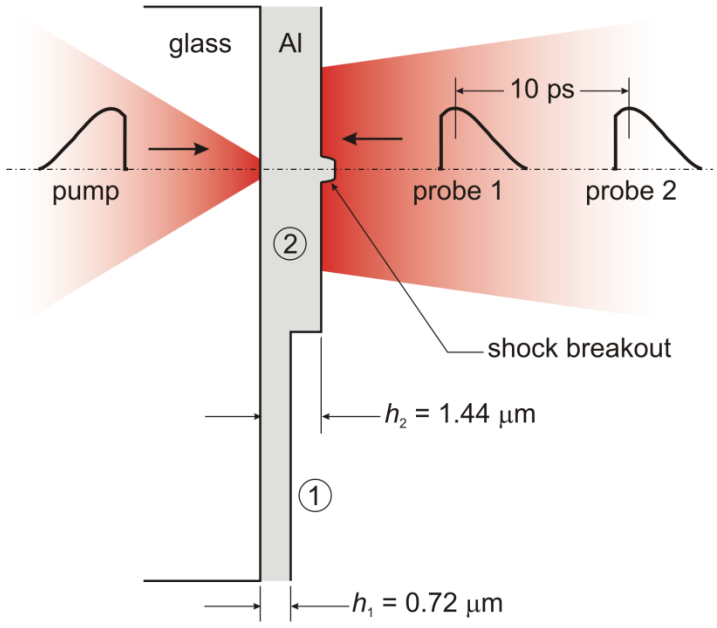

Figure 2(a).

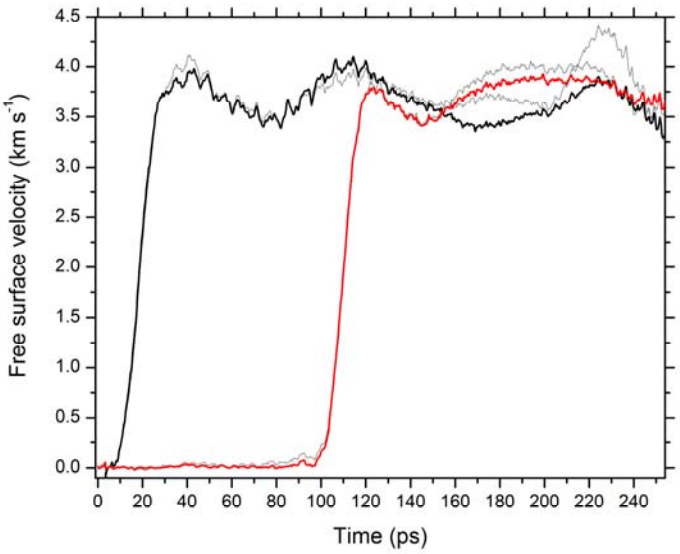

Figure 2(b).

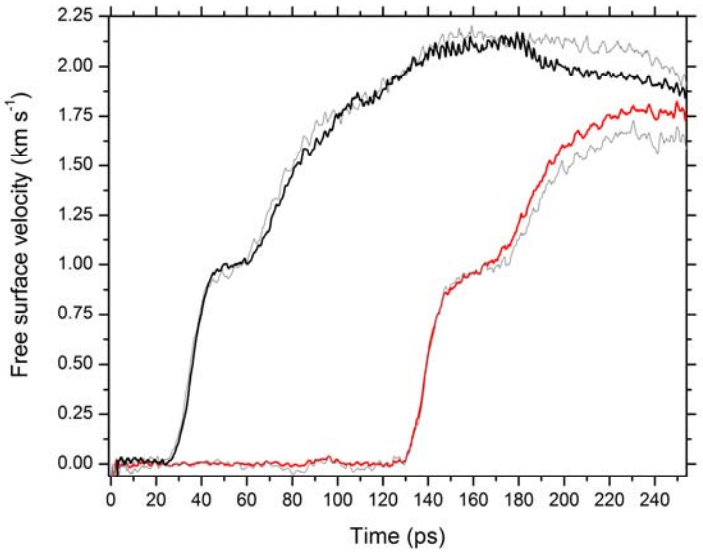

Figure 3.

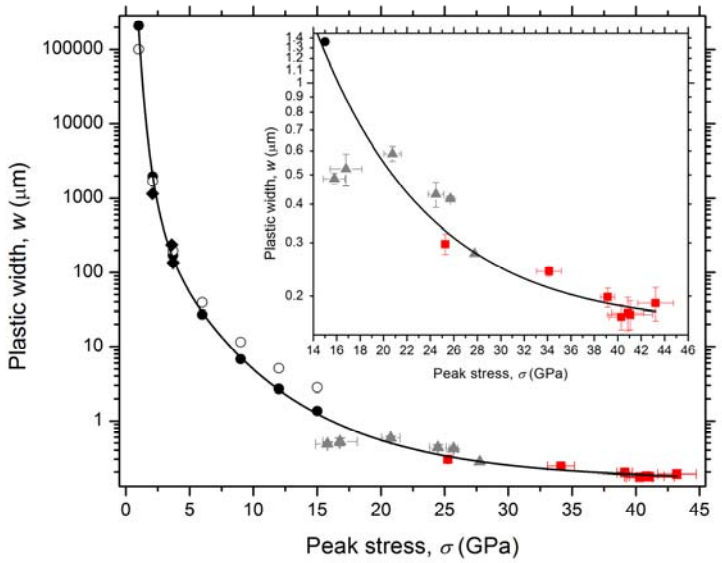

Figure 4.

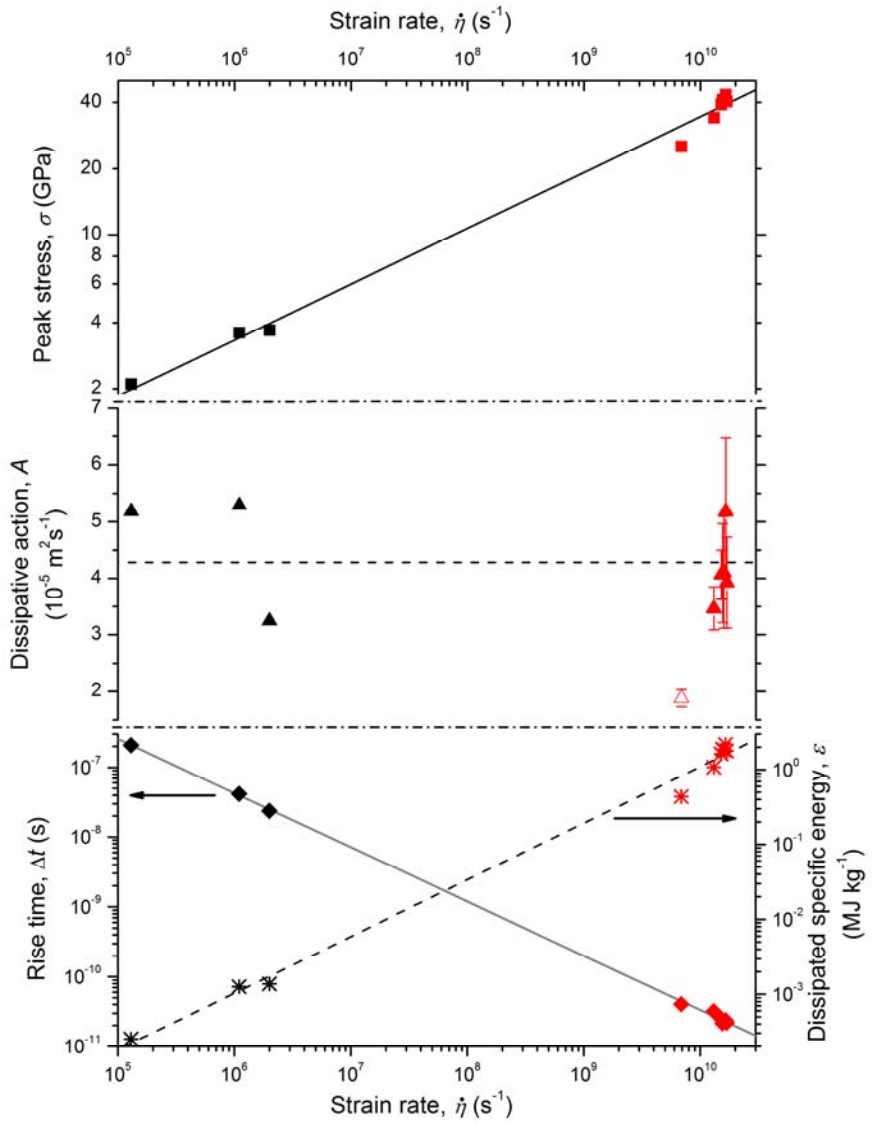
Strain rate, $\dot{\eta}$ (s^{-1})
Peak stress, σ (GPa)
Dissipative action, A (10^{-5} m^{2}s^{-1})
Rise time, Δt (s)
Dissipated specific energy, ε (MJ kg^{-1})
Strain rate, $\dot{\eta}$ (s^{-1})